PHYSICAL REVIEW A

GENERAL PHYSICS

THIRD SERIES, VOLUME 26, NUMBER 5 NOVEMBER 1982

Radial and angular correlations of two excited electrons. II. Correlations of high-lying doubly excited states

C. D. Lin

Department of Physics, Kansas State University, Manhattan, Kansas 66506

(Received 1 April 1982)

Correlations of two high-lying excited electrons are investigated in terms of simple analytical channel functions in hyperspherical coordinates. It is shown that among the N channels of $^1S^e$ states of H^- that converge to the Nth excited hydrogenic threshold, the lowest channel is always characterized by large charge densities near $r_1=r_2$ and $\theta_{12}=\pi$ at and near a certain critical hyper-radius R_c. This behavior is identical to the charge-density distribution in the Wannier theory of double electron escape near threshold for $^1S^e$ states. The different charge distributions for other higher channels are analyzed. It is shown that they do not contribute to the Wannier mechanism of threshold ionization. Properties of doubly excited states and double ionization are also discussed for other (L,S,π) values.

I. INTRODUCTION

Doubly excited states of H^- and He have recently been the subject of increasing study. In addition to the improved sophisticated calculations of position and widths of these states by many workers,[1] recent studies using hyperspherical coordinates[2,3] and group theoretical methods[4] have been aimed at revealing the nature of electron correlations of doubly excited states. Graphical display of the correlation patterns of these states has also been introduced recently.[2,5]

Hyperspherical coordinates provide a convenient basis for describing correlations. Since correlation is the property of the relative motion of two indistinguishable particles, it is natural to replace r_1 and r_2 of the usual spherical coordinates (r_1,θ_1,ϕ_1) and (r_2,θ_2,ϕ_2) by $R=(r_1^2+r_2^2)^{1/2}$ and $\alpha=\arctan(r_1/r_2)$. The correlations can be studied separately at each hyper-radius R. The distribution of charge density as a function of the angle α describes radial correlations. Its distribution as a function of the angle θ_{12} between the two electrons describes angular correlations. For spherically symmetric states, the wave functions of the two electrons are specified by $\Psi=\Psi(R,\alpha,\theta_{12})$. Correlation patterns of various doubly excited states are then revealed by the distribution of charge density on the (α,θ_{12}) plane.

In a recent article[2] (to be named I of the series), the correlation patterns of doubly excited states of H^- converging to the $N=2$ and 3 hydrogenic thresholds were investigated. This study established the importance of describing the qualitative characteristics of electron correlations for doubly excited states. Although the dramatic differences between the correlations of singly excited states and low-lying doubly excited states were observed, strong features of high-lying doubly excited states have not been investigated. In this article, the correlation pattern of these high-lying doubly excited states will be investigated.

Such a investigation is important in establishing the connection between doubly excited states and double-ionization states near threshold. In the simple one-channel problem, it is known that properties of low-lying continuum states can be related to properties of high-lying bound states. For example, single-channel quantum-defect theory relates the scattering phase shift δ_l near ionization threshold to the quantum defect σ_l of high-lying Rydberg states, $\delta_l=\pi\sigma_l$. These types of relations have also been established for multichannel problems for various types of asymptotic potentials.[6,7] The establishment of these relations is conceptually easier (but by no means trivial), since beyond the core region defined by a typical radius of the order of the size of the atom, only the motion of a single electron needs

to be considered. Beyond this radius, various excited states are characterized by the increase of the size of the states, i.e., either the size parameter or the energy of the state *alone* is adequate in describing the progression of the channel, with continuum states corresponding to the limit where the outer electron can propagate to infinity.

The increase of the size alone for doubly excited states does not lead to double ionization. In I, it was established that the correlation pattern for each channel varies in a smooth fashion with R—the charge density drops from $\alpha=45°$ as R becomes greater than R_c. Thus R_c gives the order of magnitude of the "core" radius of doubly excited states belonging to that channel. This radius R_c increases rapidly with the degree of double excitations. For R beyond a few times R_c, the radial correlation of the outer electron with the inner one is lost. (The angular correlation is maintained at large R due to the degeneracy of hydrogen-like excited states.[3]) Increase of R along the *same* channel eventually leads to *single ionization with simultaneous core excitations.* To lead to double ionization, according to the Wannier theory[8] as well as the later development of Rau[9] and Peterkop,[10] the two electrons have to maintain strong radial correlations over a large range of R. Thus, to lead to double ionization near threshold, the wave packet has to cross from one channel to another as R increases in such a way that strong radial correlation is maintained. It is important to investigate whether this channel hopping proceeds through every channel of the manifold or only through selective channels. To answer this question, it is necessary to establish the correlation patterns of high-lying doubly excited states. In this article, we will show that it appears that only a selective class of channels are important for double ionization to proceed.

The rest of this article is organized as follows. In Sec. II, a brief summary will be given on the results from I. The theoretical models used in enumerating correlations of high-lying doubly excited states will be given in Sec. III. Surface plots of the correlation pattern for the lowest channel below the Nth hydrogenic threshold will be shown in Fig. 5 at the critical radius R_c for several values of N to illustrate the behavior of the "Wannier state." Correlation patterns for the channels below the 12th hydrogenic threshold are illustrated in Fig. 6 to show the difference of charge-density distributions for high-lying channels. All the graphical displays are for $^1S^e$ of H^-. The mechanisms of double excitations and double ionizations are discussed in Sec. IV, in connection with the properties of doubly excited states studied in Sec. III.

II. SUMMARY OF CORRELATIONS FOR LOW-LYING DOUBLY EXCITED STATES

Based upon the adiabatic approximation and limiting ourselves here only to $^1S^e$ states, the two-electron wave function of H^- is expressed as

$$\Psi^n_\mu(R,\alpha,\theta_{12})=F^n_\mu(R)\Phi_\mu(R;\alpha,\theta_{12}) \tag{1}$$

for the nth state in the μth channel. We define Ψ and Φ to include appropriate phase space factors such that $|\Psi|^2$ denotes the volume charge density and $|\Phi|^2$ denotes the surface charge density on the hyperspherical surface given by $R=$const. Analogous to the Born-Oppenheimer approximation for diatomic molecules, expansion (1) introduces a potential curve $U_\mu(R)$ for each channel μ. In Fig. 1, the three potential curves that converge to the $N=3$ excited states of hydrogen atoms are shown. Notice that the lowest curve shows a deep attractive well with minimum at $R_{\min}=20$ a.u. In Fig. 2, the surface charge densities for the three channels are shown at $R=20$, 30, and 40 a.u. Detailed discussions on these plots and the method of calculations can be found in I. We only summarize two important features here.

(1) Each channel shows its own distinct correlation pattern. By denoting the channels by $\mu=(N,\lambda)$, where N refers to the dissociation limit and λ the λth channel within the manifold of chan-

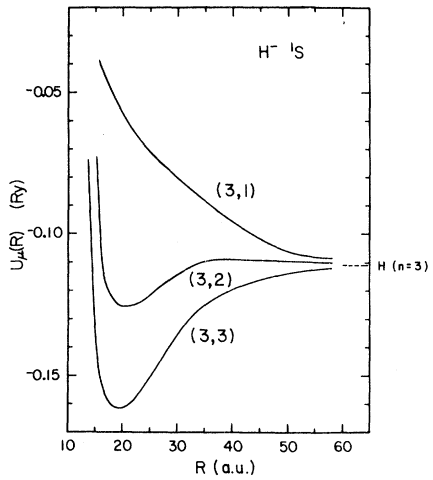

FIG. 1. Adiabatic potential curves for the three channels of H^- $^1S^e$ states that converge to the $N=3$ threshold of H.

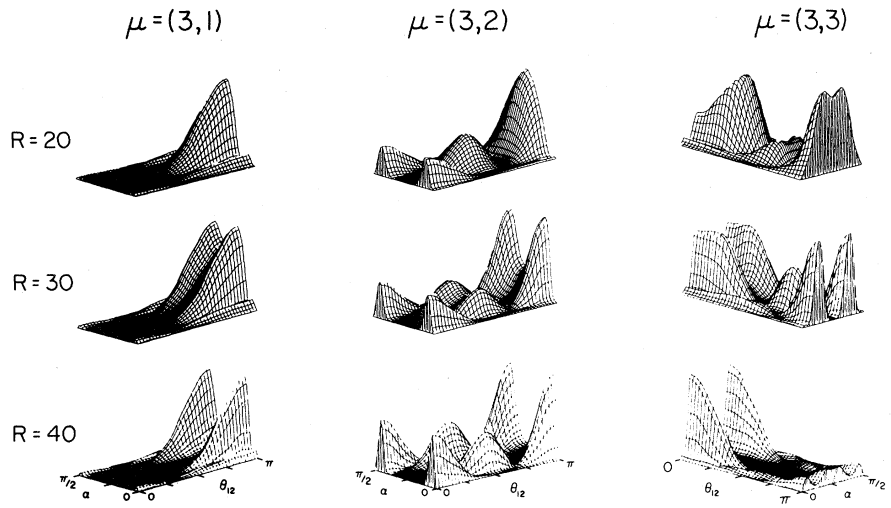

FIG. 2. Surface-charge-density plots $|\Phi_\mu(R;\alpha,\theta_{12})|^2$ for the three channels in Fig. 1 at $R=20$, 30, and 40 a.u. Notice that the graphs for the $\mu=(3,3)$ channel are oriented differently to reveal more detailed structure (adopted from Ref. 2).

nels that converges to the same limit, we notice that the lowest channel $\mu=(3,1)$ shows a large charge-density distribution for $\theta_{12}\sim 180°$, the highest channel $\mu=(3,3)$ shows a large charge concentration for $\theta_{12}\sim 0°$, and the channel in the middle $\mu=(3,2)$ shows a distinct peak of charge concentration for $\theta_{12}\sim 90°$. For $R=20$, the (3,1) channel shows a pronounced peak at $\alpha=45°$ and $\theta_{12}=180°$. (This point is to be called the Wannier point as it is important in the Wannier theory of double ionization.) This type of correlation in $\mu=(3,1)$ is similar to the symmetric stretch of a linear molecule with the nucleus in the center and the two electrons on the two sides. It might be argued that the $\mu=(3,2)$ channel has geometry like that of H_2O molecules, but this analogy is somewhat limited because the charge density is not very localized.

(2) As R increases along a given channel, the charge density along $\alpha=45°$ decreases if $R>R_c$, while the distribution on θ_{12} is relatively unchanged. In other words, deviation from $R=R_c$ implies an unstable redistribution in α while the distribution in θ_{12} is stable. This behavior is due to the nature of Coulombic interactions between two electrons and one positively charged particle. By referring to the effective charge $C(\alpha,\theta_{12})$ (such that the total potential energy is C/R) shown in Fig. 3, one notices that the potential along $\alpha=45°$ is a ridge which shows little dependence on θ_{12} except for $\theta_{12}\sim 0°$. If one electron drops below the ridge, this electron will be accelerated toward the nucleus and the other will be accelerated to large R, resulting in the loss of radial correlations. This loss of flux from the ridge prevents the two electrons from reaching large R simultaneously.

As we proceed to channels associated with higher thresholds, it is important to investigate what features are sharpened and what new features emerge.

III. CORRELATIONS OF HIGH-LYING DOUBLY EXCITED STATES

The more rigorous numerical procedures used in I are not suitable for studying high-lying doubly excited states. Even conventional configuration-mixing methods are impractical because of the large

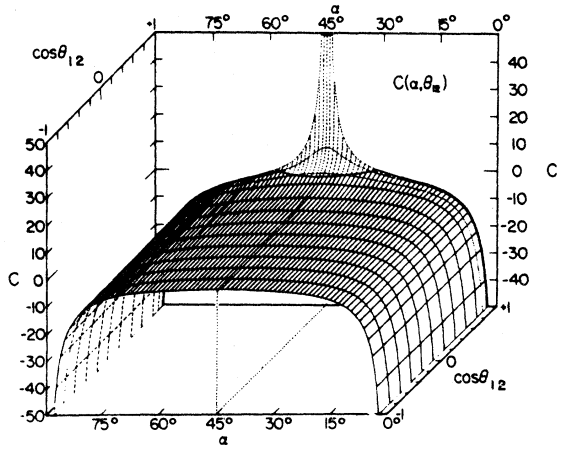

FIG. 3. Relief plot of the effective charge for H^- on the (α,θ_{12}) plane (adopted from Ref. 15).

number of Slater integrals that have to be evaluated.[11] On the other hand, based upon the simple analytical channel functions[12] described earlier, it is a simple matter to obtain approximate channel functions which can be used to study high-lying channels.

A. Approximate channel functions

Consider the $N\,{}^1S^e$ channels that converge to the Nth hydrogenic thresholds in the limit of $R\to\infty$ and $\alpha\to 0$. Because of the degeneracy of the hydrogenic excited states, the weak electric field due to the outer electron can easily mix different Nl states of the same N of the core. This mixing is easily represented in the dipole representation, where, besides the radial part of the outer electron, the wave function of the inner electron and the angular part of the outer electron is given by

$$\Phi_{N\lambda}(\vec{r}_1,\hat{r}_2)=\sum_l C_l^{N\lambda}P_{Nl}(r_1)\mathcal{Y}_{ll00}(\hat{r}_1,\hat{r}_2)\ , \quad (2)$$

where P_{Nl} is the r-weighted radial hydrogenic wave function and

$$\mathcal{Y}_{ll00}(\hat{r}_1,\hat{r}_2)=(-1)^l\left[\frac{2l+1}{4\pi}\right]^{1/2}P_l(\cos\theta_{12}) \quad (3)$$

is the coupled angular-momentum wave function of the two electrons for $L=M=0$. The coefficients $\{C_l^{N\lambda}\}$ are obtained by diagonalizing the Stark field in the $\{Nl\}$ manifold. The function given by (2) corresponds to the channel function in the limit of $R\to\infty$ and $\alpha\to 0$. To find the channel function for finite R, we follow the prescription in Ref. 12 by replacing r_1 in Eq. (2) by $R\sin\alpha\cos\alpha$ such that (2) becomes

$$\Phi_\mu(R;\alpha,\theta_{12})=\sum_l C_l^\mu N_l(R)P_{Nl}(R\sin\alpha\cos\alpha)\times(-1)^l\left[\frac{2l+1}{4\pi}\right]^{1/2}P_l(\cos\theta_{12})\ , \quad (4)$$

where $N_l(R)$ is the new renormalization constant satisfying

$$N_l^2(R)\int_0^{\pi/2}P_{nl}^2(R\sin\alpha\cos\alpha)d\alpha=1\ . \quad (5)$$

The mixing coefficients C_l^μ in (4) are *not* allowed to vary with R from the values determined in the $R\to\infty$, $\alpha\to 0$ limit. This procedure is consistent with the fact that angular correlations remain essentially constant and radial correlations are taken care by the procedure of replacing r_1 by $R\sin\alpha\cos\alpha$. In Ref. 12, it was shown that this is a valid method for $R\geq R_c$.

B. Comparison with adiabatic channel functions

The approximate channel functions calculated from Eq. (4) for the three $N=3$ channels are displayed at $R=20$, 30, and 40 in Fig. 4. By com-

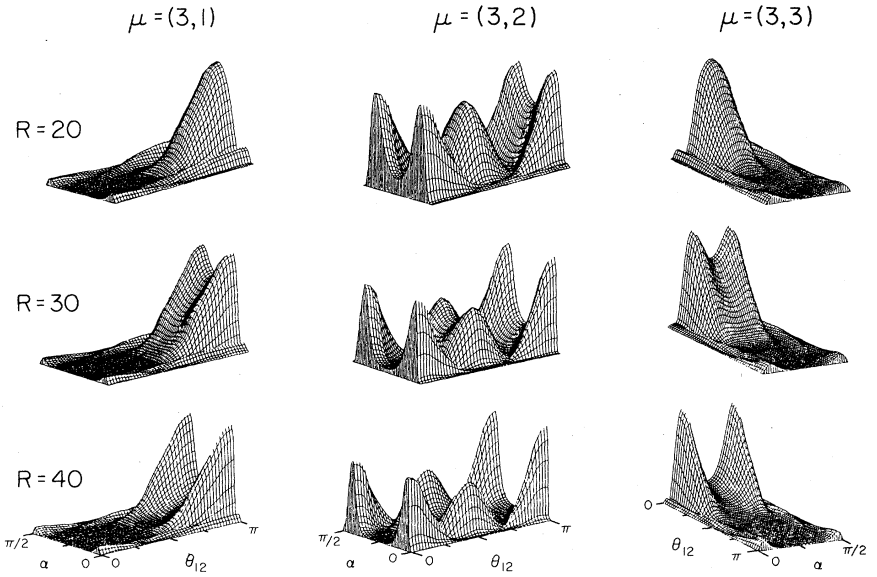

FIG. 4. Surface-charge-density plots calculated using the approximate functions given in Eq. (5). These plots are to be compared with the accurate ones shown in Fig. 2. They are shown for the same R values and for the same orientations.

paring with the graphs shown in Fig. 2, we notice that all the major features of the correlations of these channels as well as the evolution of each channel with R are well reproduced. In particular, the large peak at the Wannier point for $R=20$ (corresponding to R_c where the potential curve has the minimum) for channel (3,1) is clearly exhibited in Fig. 4. Therefore, the simple functions (4) are adequate in describing major correlation features of doubly excited states for each channel.

C. Correlations of higher $(N,1)$ and $(N,2)$ channels for H^- $^1S^e$ states

The lowest channel $(N,1)$ below each Nth excited thresholds always exhibits large charge density at the Wannier point at a certain critical radius R_c near where the potential curve has the minimum. For values of R away from R_c, the charge density at the Wannier point drops. Without actually calculating $U_\mu(R)$ with the approximate function (4), the critical radius for each $(N,1)$ channel is located by searching for R_c where $|\Phi_\mu(R;\alpha=45°, \theta_{12}=180°)|$ has the maximum. Another feature of the higher $(N,1)$ channels is the high degree of localization of charge density centered at the Wannier point for high N. In Figs. 5(a) and 5(b) the variation of $|\Phi_\mu(R_c;\alpha=45°,\theta_{12})|$ with θ_{12} and of $|\Phi_\mu(R_c;\alpha,\theta_{12}=\pi)|$ with α are shown at the critical radii R_c for several $(N,1)$ channels. The absolute value of $\Phi_\mu(R_c;\alpha=45°,\theta_{12}=180°)$ increases rapidly with increasingly higher-N channels. The half-width in θ_{12} and in α decreases with increasing N. Therefore, we notice that along the $(N,1)$ channels the electron correlation for each channel at the critical radius is such that the two electrons are to maintain at the same distance from the nucleus and on opposite sides of the nucleus. Deviations of the charge distribution from the "equilibrium point" $r_1=r_2$ and $\theta_{12}=180°$ become smaller with increasing N.

To get a more complete view of the charge-density distributions, the surface plots of $|\Phi_\mu(R_c;\alpha,\theta_{12})|^2$ are shown in Fig. 6 for $(N,1)$ channels with $N=4$, 6, 8, 10, and 12 at their corresponding critical radii R_c^N. To compare the behavior with other channels, the corresponding $(N,2)$ channels are also shown at the same R_c^N. In Fig. 6, all the graphs are normalized to have the same maximum height. Since $|\Phi_\mu(R_c;\alpha,\theta_{12})|^2$ is normalized to unity on the hyperspherical surface, plots with narrow features actually have sharp peaks and plots with broad features actually have

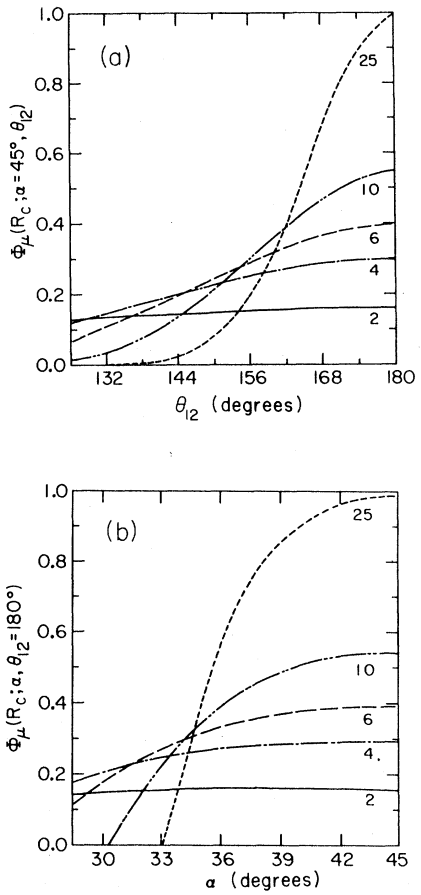

FIG. 5. Variation of $|\Phi_\mu(R_c;\alpha=45°,\theta_{12})|$ with θ_{12} and $|\Phi_\mu(R_c;\alpha,\theta_{12}=\pi)|$ with α for the $\mu=(N,1)$ channels for $N=2$, 4, 6, 10, and 25. These graphs illustrate the high-degree localization of α and θ_{12} for the $(N,1)$ channels around the Wannier point for higher values of N.

broader charge distributions. For each $(N,1)$ channel shown in Fig. 6, the R_c^N value and the charge density at the Wannier point are given on the left of the graph. For $N=2$, 4, 6, 8, 10, 12, and 25, the peak charge densities (the critical radii R_c^N) are 0.026 (6.4), 0.086 (39), 0.155 (102), 0.230 (195), 0.309 (320), 0.390 (470), and 0.986 (2230). We notice that as N increases, the plots are similar except that the rise to the peak values is faster for high N. The plots for $(N,2)$ channels are broader in α. The $(N,1)$ channels show no nodal lines in θ_{12} coordinate, while the $(N,2)$ channels show *one* nodal line in the θ_{12} coordinate. All the doubly excited channels show nodal lines in the α coordinate. For $R>R_c$, these nodes in α shift to smaller values of α (as well as to α close to 90° from the symmetry condition).

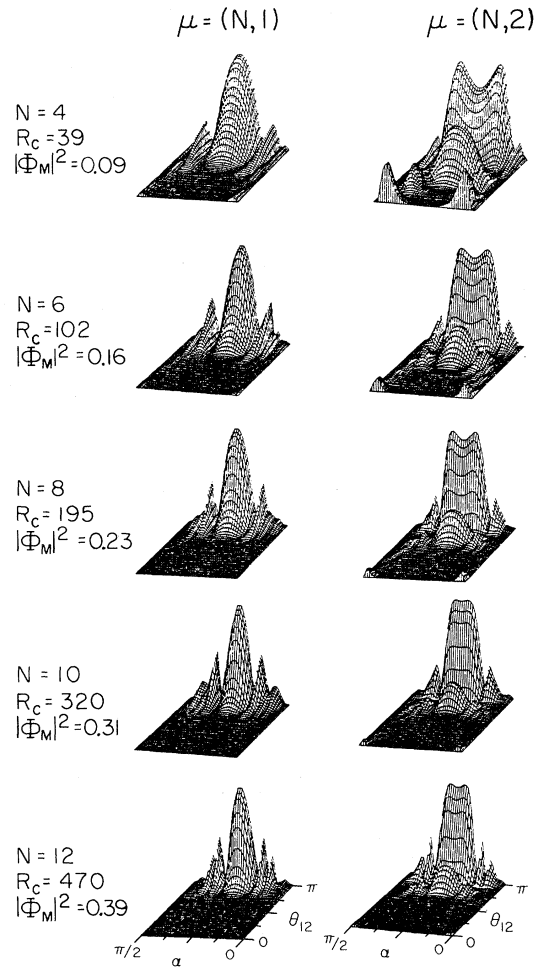

FIG. 6. Surface-charge-density plots for the $(N,1)$ and $(N,2)$ channels for $N=4$, 6, 8, 10, and 12. Critical radius for each $(N,1)$ channel and its charge density at the Wannier point is given on the left of the graph. All the graphs shown are normalized to have the same maximum height. Plots with narrow features indicate sharper localization of the charge distribution.

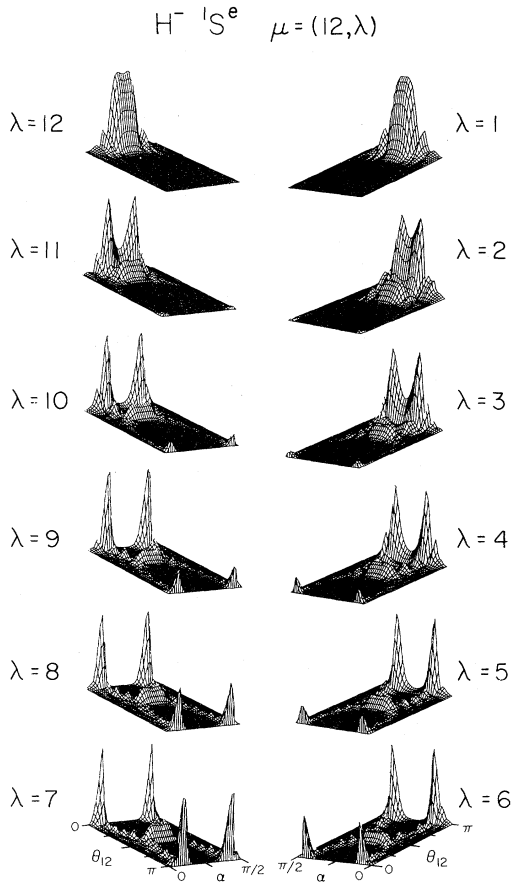

FIG. 7. Surface-charge-density plots for the 12 channels of H^- $^1S^e$ states that converge to the 12th hydrogenic thresholds. To illustrate the "mirror" symmetry, the channels are positioned in the way shown. Notice that the orientations of the graphs between the two columns are different.

D. Correlations of doubly excited states of H^- below the $N=12$ threshold

To appreciate the correlation pattern of high-lying doubly excited states, in Fig. 7 the surface charge densities of the 12 channels below the 12th hydrogenic threshold of H for $^1S^e$ states of H^- are shown at $R=500$ a.u. The channels are labeled as $(12,\lambda)$ where higher values of λ correspond to more repulsive channels. We notice that the correlation patterns among the λ channels with fixed N for $^1S^e$ states differ mainly in the angular correlations. The lowest channel has a charge distribution that is concentrated in the large θ_{12} region and the highest channel has a large charge distribution in the small θ_{12} region. On the other hand, radial correlation *does* come into play also. Small Coulomb repulsion between the two electrons favors $\alpha \neq 45°$ if $\theta_{12} \sim 0°$. Thus, except for the highest $\lambda=12$ channel, all the higher channels stay away from the region $\alpha \sim 45°$ in the small θ_{12} region. Successive higher λ channels acquire more nodal lines in the θ_{12} coordinate. Besides that, the surface charge distribution on the (α,θ_{12}) plane appears to exhibit "mirror symmetries" in the manner displayed in Fig. 7.

E. Correlations of doubly excited $^3S^e$ states

The differences between $^1S^e$ and $^3S^e$ doubly excited states are primarily due to "Pauli exchange

correlations," i.e., due to the fact that $^1S^e$ state wave functions are even functions and $^3S^e$ wave functions are odd functions with respect to the reflection at $\alpha=45°$. In the present approach, this exchange correlation is reflected as radial correlation in that $^3S^e$ wave functions always vanish at $\alpha=45°$. For angular correlations, $^1S^e$ and $^3S^e$ states of similar channels are essentially the same. Therefore, the correlation patterns between the corresponding channels are similar except for the fixed nodal line along $\alpha=45°$ for $^3S^e$ channels. These behaviors have been examined in I for low-lying doubly excited states and should remain true for high-lying doubly excited states as well.

Because of the nodal line along $\alpha=45°$, the charge densities does not have a maximum at the Wannier point for $(N,1)$ channels of $^3S^e$ states. The absence of charge density along $\alpha=45°$ results in the hypothesis that $^3S^e$ states are not important for describing double ionization near threshold (see Sec. IV).

F. Correlation of doubly excited $^1P^o$ and $^3P^o$ state

Correlations of states with $L\neq 0$ are more difficult to display graphically since the wave functions not only depend on R, α, and θ_{12}, but also depend on Euler angles which describe the overall rotations. Unlike diatomic molecules, the rotational motion in the two-electron atoms cannot be separated from the description of electron correlations. It is possible to integrate over the overall rotation angles to obtain charge densities of the states on the (α,θ_{12}) plane, but this subject will be investigated in the future.

Recall in Sec. III E we noticed that $^1S^e$ and $^3S^e$ states differ essentially only in radial correlations. For $L\neq 0$ states, the situation is complicated by the strong coupling between radial and angular correlations. Consider the description of $1snp\,^1P^o$ and $1snp\,^3P^o$ states in the independent-particle approximation; the channel functions are expressed as[13]

$$\cos\theta_1 f(R;\alpha)\pm\cos\theta_2 f\left[R;\frac{\pi}{2}-\alpha\right] \tag{6}$$

for states with $M=0$ where $+$ $(-)$ refers to singlet (triplet) states. The $+$ and $-$ combination in (7) dictates a large degree of radial and angular correlations, to be called "Pauli correlations," which have not been discussed in the literature. Consider the channel function (6) at $\alpha=45°$. It reduces to $f(R;\alpha=45°)(\cos\theta_1\pm\cos\theta_2)$. For $^1P^o$, this function vanishes when $\theta_1=\pi-\theta_2$ and peaks at $\theta_1=\theta_2$, i.e., Pauli correlation forces the two electrons to peak at $\theta_{12}\sim 0°$ and to stay away from $\theta_{12}\sim 180°$. On the other hand, for $^3P^o$ states, the function in (6) has the peak at $\theta_{12}\sim 180°$ and vanishes at $\theta_{12}\sim 0°$. This Pauli correlation explains why the energy of $1snp\,^3P^o$ state is always lower than the energy of $1snp\,^1P^o$ states since $\theta_{12}\sim 180°$ reduces the electron-electron repulsion. This type of correlation is not important when $\alpha\sim 0°$ (or $\alpha\sim 90°$) as one or the other term in (6) dominates.

For doubly excited states with nonzero L, there are also the so-called $+$ and $-$ correlations first discussed by Cooper *et al.*[14] These types of correlations were examined by Lin[15] in terms of radial correlations within each $[l_1 l_2]$ pair of the partial-wave decomposition of the total wave function. It was noted that if both l_1 and l_2 are less than $N-1$, where N is the Nth excited hydrogen state, then there are two channels within that $[l_1 l_2]$ subspace, one with the $+$ character where $f(R;\alpha)$ shows an antinode near $\alpha\sim 45°$ and the other with the $-$ character where $f(R;\alpha)$ shows a node near $\alpha\sim 45°$. Therefore, the difference between $+$ and $-$ for $L\neq 0$ states (irrespective of the spin S) is similar to the difference between $^1S^e$ and $^3S^e$ states, i.e., mainly in radial correlations. In fact, the ratio of decay widths for $+$ to $-$ states is about the same as the ratio of decay widths for $^1S^e$ to $^3S^e$ states.

The actual correlations for doubly excited states with nonzero L are complicated by the angular correlations which mix different $[l_1 l_2]$ subspaces and by Pauli correlations which further mix radial and angular correlations to distinguish singlet from triplet states. At large hyper-radius R within a single channel (and with $\alpha\to 0$ or $\alpha\to 90°$), $+$ and $-$ correlation and the Pauli correlation become insignificant; only angular correlations remain important. These variations of correlations with R determine the properties of doubly excited states for states with nonzero L.

IV. CONNECTION WITH THE WANNIER THEORY OF THRESHOLD IONIZATION

In Sec. I, the mechanism of populating doubly excited states and of double ionization was discussed. Both high-lying doubly excited states and double-electron escape at low energies are characterized by two slow electrons where strong correlations are expected to develop because of the long-range forces and the large time of interaction over which correlations can develop. According to the Wannier theory of threshold ionization, double-electron es-

cape near threshold is possible only if the two electrons remain roughly at the same distance from the nucleus in the escape process. Referring to Fig. 3 for the effective charge $C(\alpha,\theta_{12})$, deviation of α from 45° results in a more complete screening of the nucleus by the inner electron such that the inner electron takes away most of the available energy to make double escape impossible.

The mechanism of populating high-lying doubly excited states essentially has to proceed in the same manner. In terms of the family of adiabatic potential curves within a given L and S, this means that "direct excitation" to these high-lying doubly excited states from the low-lying channels is most likely impossible.[15] Instead, these states are more likely populated through *successive* "channel hopping" from the lower channels. Recall in Figs. 2 and 4, as well as in the graphs shown in I, the charge-density distribution near $\alpha\sim45°$ for each adiabatic channel drops gradually as R becomes greater than R_c, i.e., the charge density on the potential ridge (of Fig. 3) begins to slide into the two valleys for $R>R_c$. On the other hand, there are some fractions which will not follow the adiabatic evolution and instead remain on the potential ridge and propagate to higher channels with increasing R. Therefore, in this model, channel hopping occurs through the splitting of the charge density at the potential ridge. This process of populating high-lying double excited states and double-electron escape near the threshold is called here the Wannier mechanism. Channels which do not possess significant charge densities at or near $\alpha=45°$ are thus not populated by this Wannier mechanism in the excitation process. Experimental results and theoretical calculations appear to indicate that the Wannier mechanism is the dominant one for low-energy collisions. For example, recent photoionization measurements of He below the $He^+(N)$ threshold for $N=3$, 4, and 5 by Woodruff and Samson[16] clearly indicate that there is only one channel below each N which is predominantly excited in the photoabsorption process. Recall that there are $2N-1$ channels below the $He^+(N)$ threshold for $^1P^o$ states, but most of these channels are not excited in the photoabsorption process except for the $(N,1)$ channel. Similar results were also observed for the photodetachment measurements of H^- below $H(N=3)$ (Ref. 17) and $H(N=6)$ (Ref. 18) thresholds where only states belonging to the lowest channel out of the possible five for the $H(N=3)$ manifold and the possible eleven for the $H(N=6)$ manifold are populated. These lowest channels are all distinguished by the large charge-density distribution at $\alpha=45°$ near its critical radius R_c^N. Other states belonging to the higher-λ channels of the N manifold are marked by near-zero charge densities near the potential ridge $\alpha=45°$ and are not easily excited in the collision.

In the discussion above, nothing has been said about angular correlations. Since the potential surface is essentially flat in θ_{12}, except near the singular point at $\alpha=45°$ and $\theta_{12}=0°$, deviation of θ_{12} from 180° does *not* result in any significant loss of flux from the ridge. Although the $^1S^e$ states belonging to the lowest channel in the excited $H(N)$ manifold exhibit strong angular correlation with a peak at $\theta_{12}=180°$, the fact that this peak occurs at $\theta_{12}=180°$ but not at other angles is not essential to the Wannier mechanism of populating doubly excited states, nor is it essential to the double-escape process.[19] The Wannier mechanism requires large nonzero charge density for $\alpha\sim45°$ without specifying the θ_{12} dependence. Only $^3S^e$ and $^1P^e$ states possess zero charge densities for *all* the channels at $\alpha=45°$ due to Pauli exchange correlations.[20] Thus, doubly excited states belonging to $^3S^e$ and $^1P^e$ are not easily excited and they are not important in the Wannier theory of double-electron escape. *All* other L and S states have one channel below each $H(N)$ manifold (corresponding to the one which has the deepest potential well) which has large nonzero charge densities near $\alpha=45°$ at a certain critical radius. Doubly excited states associated with these channels are often excited in the collision and they all have the same Wannier exponent for threshold ionization. Because the θ_{12} distribution depends on L and S, angular correlation between the two ionized electrons near the threshold will be different for different L and S. For example, $^1P^o$ states always have zero charge density at $\alpha=45°$ and $\theta_{12}=180°$ because of Pauli exchange correlations, thus the angular correlation between two ionized slow electrons will show a dip at $\theta_{12}=180°$.[19] On the other hand, for $^3P^o$ states, the angular correlation between two ionized slow electrons will show a maximum at $\theta_{12}=180°$ because the Pauli exchange correlation favors $\theta_{12}=180°$.

V. SUMMARY

In this article the characteristics of electron correlations of high-lying doubly excited states are examined. It is found that the systematics of correlation patterns of these high-lying channels are very similar to those of the low-lying channels studied

earlier except that the major features of each channel are sharpened. For the $N\,^1S^e$ channels of H^- that converge to the Nth hydrogenic threshold, the lowest channel is shown to have large charge concentration near $\theta_{12}\sim 180°$. Other channels of the N manifold are marked by their charge distribution at smaller θ_{12}, with the higher channel (within the N manifold) having charge concentration at smaller θ_{12}.

The lowest $(N,1)$ channels for each N are singled out as the major important channels that can be populated in a *slow* collision. These channels are shown to exhibit large charge density peaked around the Wannier point ($\alpha=45°$ and $\theta_{12}=180°$) at and near the critical radius R_c^N characteristic of that $(N,1)$ channel. As N increases, the critical radius R_c^N increases and the rise to the Wannier peak becomes sharper. Within a given $(N,1)$ channel, as R becomes greater than R_c^N, the peak gradually shifts to $\alpha=45°\pm\beta$, where β increases with R. In other words, for $R>R_c^N$, the charge distribution within the $(N,1)$ channel begins to slide away from the potential ridge (of Fig. 3) into the two valleys. On the other hand, through channel hopping to the next $(N+1,1)$ channel, some fraction of the charge densities will be transferred to the $(N+1,1)$ channel. Between R_c^N and R_c^{N+1}, it appears that the increase of R is to focus the charge density in the $(N+1,1)$ channel to the vicinity of $\alpha=45°$. As $R>R_c^{N+1}$, the charge density that remains in the $(N+1,1)$ channel will diverge from $\alpha=45°$. This process of transferring flux from one $(N,1)$ channel to the next $(N+1,1)$ channel successively appears to be the major mechanism of populating high-lying doubly excited states and is consistent with the Wannier mechanism of double ionization near threshold. This mechanism is consistent with available experimental data on high-lying doubly excited states and threshold ionization.

From the analysis of the correlations of doubly excited states belonging to other L and S, it is argued that angular correlation plays no significant role in the Wannier mechanism. This mechanism requires only that the relevant channels have charge densities peaking at $\alpha=45°$ and *some* θ_{12} at their corresponding critical radii. The effectiveness of the Wannier mechanism is expected to be independent of θ_{12}. Therefore, except for $^3S^e$ and $^1P^e$ states, where all the channel functions have a nodal line along $\alpha=45°$ (because of Pauli exchange symmetry), all other L and S symmetries have one class of channels which behave similar to the $(N,1)$ channels in $^1S^e$. Within the many channels that converge to the Nth excited hydrogenic thresholds, the important channel again will be the one which has the most attractive potential curve.

ACKNOWLEDGMENTS

The author would like to thank Dr. M. H. Day, Dr. U. Fano, Dr. C. H. Greene, Dr. A. R. P. Rau, and Dr. A. F. Starace for their critical comments on the manuscript. This work is supported in part by the Department of Energy, Division of Chemical Science and in part by the Alfred P. Sloan Foundation.

[1]A. J. Taylor and P. G. Burke, Proc. Phys. Soc. London 92, 336 (1967); P. G. Burke, A. J. Taylor, and S. Ormonde, *ibid.* 92, 345 (1967); K. T. Chung and J. C. Y. Chen, Phys. Rev. A 6, 686 (1972); A. K. Bhatia and A. Temkin, *ibid.* 8, 2184 (1973); G. W. F. Drake and A. Dalgarno, Proc. R. Soc. London, Ser. A 320, 549 (1971); J. T. Broad and W. P. Reinhardt, Phys. Rev. A 14, 2159 (1976); Y. K. Ho, J. Phys. B 12, L543 (1979); L. A. Morgen, M. R. C. McDowell, and J. Callaway, *ibid.* 10, 3297 (1977).

[2]C. D. Lin, Phys. Rev. A 25, 76 (1982). This paper is referred as article I of this series.

[3]C. D. Lin, Phys. Rev. A 25, 1535 (1982).

[4]D. R. Herrick and M. E. Kellman, Phys. Rev. A 21, 418 (1980); M. E. Kellman and D. R. Herrick, *ibid.* 22, 1536 (1980).

[5]H. Y. Yuh, G. Ezra, P. Rehmus, and R. S. Berry, Phys. Rev. Lett. 47, 497 (1981).

[6]C. Greene, U. Fano, and G. Strinati, Phys. Rev. A 19, 1485 (1979).

[7]M. Gailitis and R. Damburg, Proc. Phys. Soc. London 82, 192 (1963).

[8]G. Wannier, Phys. Rev. 90, 817 (1953).

[9]A. R. P. Rau, Phys. Rev. A 4, 207 (1971).

[10]R. Peterkop, J. Phys. B 4, 513 (1971).

[11]F. Iachello and A. R. P. Rau, Phys. Rev. Lett. 47, 501 (1981).

[12]C. D. Lin, Phys. Rev. A 23, 1585 (1981).

[13]P. M. Morse and H. Feshbach, *Methods of Theoretical Physics* (McGraw-Hill, New York, 1953), Part II, p. 1728.

[14]J. W. Cooper, U. Fano, and F. Prats, Phys. Rev. Lett. 10, 518 (1963).

[15]C. D. Lin, Phys. Rev. A 10, 1986 (1974).

[16]P. R. Woodruff and J. A. R. Samson, Phys. Rev. A 25, 848 (1982).
[17]M. E. Hamm *et al.*, Phys. Rev. Lett. 43, 1715 (1979).
[18]D. Clark and H. Bryant (private communication).
[19]C. H. Greene and A. R. P. Rau, Phys. Rev. Lett. 48, 533 (1982).
[20]C. H. Greene, Phys. Rev. Lett. 44, 869 (1980); U. Fano and C. H. Greene, Phys. Rev. A 22, 1760 (1980).